

Article

Characteristics of Overburden and Ground Failure in Mining of Shallow Buried Thick Coal Seams under Thick Aeolian Sand

Guangchun Liu ^{1,2} , Youfeng Zou ¹, Wenzhi Zhang ^{1,*} and Junjie Chen ¹

¹ School of Surveying and Land Information Engineering, Henan Polytechnic University, Jiaozuo 454000, China; liugh168@home.hpu.edu.cn (G.L.); zouyf@hpu.edu.cn (Y.Z.); chenjj@hpu.edu.cn (J.C.)

² School of Resources and Civil Engineering, Liaoning Institute of Science and Technology, Benxi 117004, China

* Correspondence: zhangwenzhi@hpu.edu.cn

Abstract: Mining can lead to overburden failure and ground damage, which are more severe in mining shallow buried thick coal seams (SBTCS) under thick aeolian sand (TAS). We attempted to discover characteristics of mining in this particular geological condition through theoretical derivation and numerical simulation, and field monitoring. Theoretical methods, combined with numerical simulation and field monitoring methods, reveal the essence of the development and distribution of surface cracks caused by mining SBTCS and depth to thickness ratio (DTR) to be 13.43, less than 15. The findings show that, when mining SBTCS, the overburden breaks down periodically, the initial collapse distance is greater than the collapse step, approximately 55 m on average, and the collapse step is approximately 45 m, on average, in the Daliuta Coal Mine. The collapsed blocks are stacked into goaf and form “masonry beams”, and many cracks and pores are generated between the blocks. The weak stress of the aeolian sand layer causes the movement angle in the aeolian sand layer to be smaller than that in the bedrock, and leads to much shear, tension and compression failure on the ground, and the main forms of cracks are compression uplift, tensile cracking, shear step.



Citation: Liu, G.; Zou, Y.; Zhang, W.; Chen, J. Characteristics of Overburden and Ground Failure in Mining of Shallow Buried Thick Coal Seams under Thick Aeolian Sand. *Sustainability* **2022**, *14*, 4028. <https://doi.org/10.3390/su14074028>

Academic Editors: Longjun Dong, Yanlin Zhao and Wenxue Chen

Received: 12 February 2022

Accepted: 23 March 2022

Published: 29 March 2022

Publisher's Note: MDPI stays neutral with regard to jurisdictional claims in published maps and institutional affiliations.



Copyright: © 2022 by the authors. Licensee MDPI, Basel, Switzerland. This article is an open access article distributed under the terms and conditions of the Creative Commons Attribution (CC BY) license (<https://creativecommons.org/licenses/by/4.0/>).

Keywords: thick aeolian sand; shallow buried thick seam; overburden failure; ground damage; numerical simulation

1. Introduction

After a coal seam is mined out from underground, the rock stratum above the goaf is affected by mining, resulting in collapses, cracks, and surface subsidence, water level decline, ecological environment deterioration, and so on [1–3]. When mining shallow buried thick coal seams (SBTCS), these phenomena and the damage are more serious and faster [4]. The main areas of coal exploitation in China have been transferred from east to west. Northwest China is enriched in coal with shallow buried, thick coal seams and simple overburden geological conditions [5]. The Daliuta Coalfield, in northern Shanxi Province, China [6], is located under a thick aeolian sand (TAS) layer of Quaternary sediment, mainly aeolian sand [7]. This is a typical coal seam occurrence condition with SBTCS. There are numerous problems associated with mining SBTCS, especially under TAS layers. After the coal seam is mined, a roof of coal collapse can cause grave damage to the overburden and ground covered by the aeolian sand [8–10]. Ground subsidence and cracks are another critical issue [11–13]. Many experts and scholars have conducted research on this problem of mining SBTCS and have achieved rich results. FAN De-yuan and others integrated physical and mechanical tests, theoretical analysis, similar material tests, numerical calculations, on-site industrial tests and other methods [14,15]. They systematically studied the deformation mechanism of the surrounding rock in mining under TAS and thick coal seam (TCS). They established a mechanical analysis model for the surrounding rock. The change in the regular pattern of displacement, stress, energy and other parameters were analyzed [16,17]. These studies did not consider thin, overburden and shallow burials. A numerical simulation method has been used to study the design of a retaining coal pillar width in mining SBTCS

to ensure mining safety and improve coal yield [18–21]. Behrooz Ghabraie and others established a stress model and calculated and analyzed the stress related problems of mining TAS and TCS. According to the data of surface settlement monitoring and the geomechanical parameters of geological boreholes, the relevant parameters of the numerical model are corrected and adjusted. Numerical simulation and engineering analysis have established a mechanical theoretical basis for SBTCS [22–24]. Through theoretical derivation and numerical simulation analysis, Booth and others studied the surface deformation caused by overburden failure in mining SBTCS under TAS and established a prediction model for subsidence [25,26]. The existing prediction methods for mining subsidence cannot correctly explain deforming ground undulations. The research focuses on surface subsidence. Li Meng and others aimed at the complex conditions of ground undulations. Through similar material tests and numerical simulation analysis, a new prediction method for overburden movement was proposed based on key stratum theory and the rock Mohr–Coulomb failure criterion [15,27,28]. According to the occurrence characteristics of SBTCS, Park and others systematically studied the development and evolution regulations of overburden failure in shallow buried coal seams by using a similar 3D material physical test method. Ground subsidence of the SBTCS is mainly caused by aeolian sand layer settlement and bedrock breakage. The length and advancing distance of the workface directly affect the displacement of the surface and overburden [10].

However, most of the above research is mainly aimed at SBTCS with burial depths greater than 150 m, and depth (burial depth of coal seam) to thickness (thickness of coal seam) ratios (DTR) are more than 15 ($H/h > 15$). Some of them focus on TCS or TAC separately. Some scholars have used similar methods of test analysis, a small error can be amplified dozens or even hundreds of times because of the similarity ratio. Others have established corresponding mechanics based on the movement characteristics of the overburden. This method is based on theoretical calculation, and the essence of overburden failure can be obtained. Using the numerical simulation method based on theoretical calculations, the characteristics and regular pattern of overburden failure can be obtained [29]. In this study, the buried depth of SBTCS is approximately $H = 90$ m, and thickness of coal is $h = 6.7$ m (DTR = 13.43, less than 15) [30]. The thickness of aeolian sand is 38.5 m, accounting for approximately 42.6% of the buried depth, which is located in the Daliuta mine. According to the theory of the key stratum, the mechanical model of a key stratum collapse was established, and the initial failure distance and periodic failure distance of the key stratum were calculated. The model was verified by numerical simulation. This paper discusses the characteristics of overburden failure with mining SBTCS under TAS. It explains the ground damage characteristics and cracks development.

2. Materials and Methods

Academician Qian Minggao and others proposed the key stratum theory [31,32]. Due to the difference in thickness and properties of each rock layer in the overburden, its control and support of various overburdened rock strata are significantly different. The thickness and elastic modulus of the key stratum are large, and the strength is stronger than that of the other strata. The subsidence of key stratum is synchronous and coordinated in all or part of the upper overburden. Before the key stratum breaks, a slab or beam is formed to bear the weight of the upper rock. When it fails, it can continue to support the upper overburden with a “cantilever beam” as shown in Figure 1.

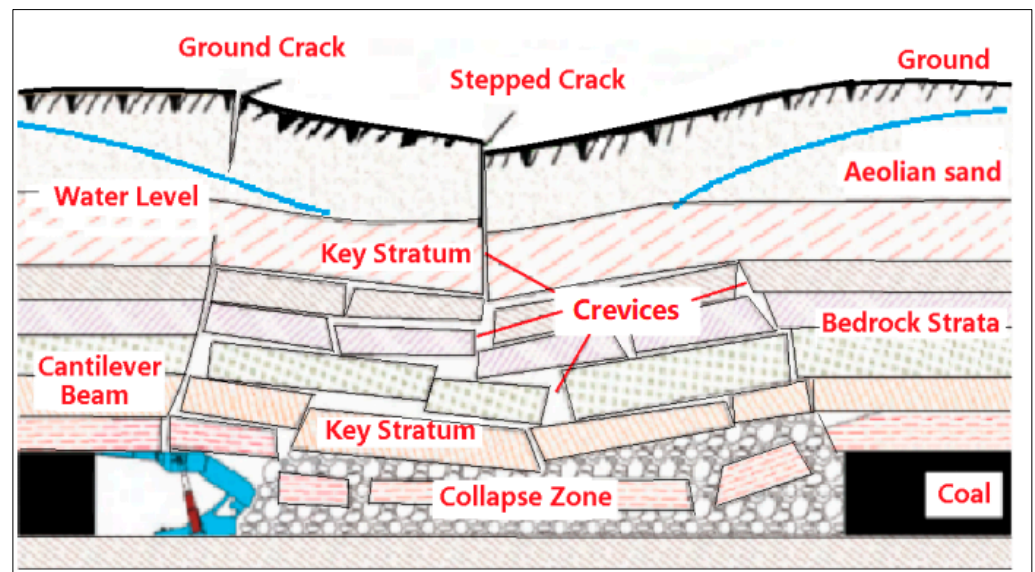


Figure 1. Schematic diagram of ground damage and of key stratum in overburden failure.

The overburden is simplified into a calculation model to analyze the failure principle of the key stratum. Assuming the bedrock layer of the overburden has n ($n > 2$) layers, the upper part of the bedrock is an aeolian sand layer with weak bearing capacity, and its load is q . According to the key stratum theory, the first key stratum controls and bears all the overburden and key stratum above, and it simultaneously coordinates deformation [33].

The following formula holds:

$$\frac{M_1}{E_1 I_1} = \frac{M_2}{E_2 I_2} = \frac{M_3}{E_3 I_3} = \dots = \frac{M_i}{E_i I_i} \quad (1)$$

In the formula:

M_i is the bending moment of the i -th rock layer;

E_i is the elastic modulus of the i -th rock layer;

I_i is the inertia moment of the i -th rock layer.

According to the initial in situ stress conditions and the theory of key stratum, the first key stratum of overburden $1 \sim m$ ($m < n$) layers can be regarded as a composite rock beam structure, and its bending moments are:

$$M_a = M_1 + M_2 + M_3 + \dots + M_m = \sum_{i=1}^m M_i \quad (2)$$

Similarly, the second key stratum of the overburden $m + 1 \sim n$ ($m < n$) layers can be regarded as a composite rock beam structure, and its bending moments are:

$$M_b = M_{m+1} + M_{m+2} + M_{m+3} + \dots + M_n = \sum_{i=m+1}^n M_i \quad (3)$$

After transforming Formula (1), the relationship between the first key stratum and others is established, and then brought into Formula (2):

$$M_1 = \frac{E_1 I_1 M_a}{\sum_{i=1}^m E_i I_i} \quad (4)$$

Similarly, the second key stratum of the overburden $m + 1 \sim n$ layers can be expressed as:

$$M_{m+1} = \frac{E_{m+1} I_{m+1} M_b}{\sum_{i=m+1}^n E_i I_i} \quad (5)$$

When the mining distance is small, the stress of the first and second key stratum does not reach the destruction level, and the key stratum does not collapse. When the workface continues to advance and reaches the limit collapse distance, the first and second key stratum collapse simultaneously. With the workface advancing, the key stratum will collapse periodically. The key stratum block stacks into the collapse zone to form a “masonry beam”. There are numerous large pores and crevices between the blocks.

Calculating the bearing capacity of the key stratum is usually carried out by using the recursive method. First, suppose that, when the first key stratum only controls itself, the load it bears is q_1 ; then, it can be calculated by Formula (6):

$$q_1 = \gamma_1 h_1 \quad (6)$$

In the formula, h_1 represents the gravity density and thickness of the rock layer.

Second, when the first key stratum can bear the first and second layers, the load to be borne is q_2 , and then it can be calculated by the Formula (7):

$$q_2 = \frac{E_1 h_1^3 (\gamma_1 h_1 + \gamma_2 h_2)}{E_1 h_1^3 + E_2 h_2^3} \quad (7)$$

Next, recursively, the bearing capacity q_m of the m -th stratum can be obtained [34], which can be calculated by Formula (8):

$$q_m = \frac{E_m h_m^3 (\sum_{i=m}^n \gamma_i h_i + q)}{\sum_{i=m}^n E_i h_i^3} \quad (8)$$

In the formula:

h_m represents the thickness of the combined key stratum m ;

E_m represents the elastic modulus of the combined key stratum m ;

h_i is the i -th rock layer thickness.

According to the characteristics of the rock beam in the key layer theory, the coordinates are established as shown in Figure 2. To simplify the calculation, the broken distance of the key stratum is calculated using the fixed bracket mechanism model. The center of the rock beam and the left boundary of the rock beam are the origin, the positive direction of the X axis is horizontal to the right, and the positive direction of the Y axis is vertically upward. The length of the rock beam is L , the thickness is h , and the uniform load q of the loose layer is applied to the upper part of the rock beam.

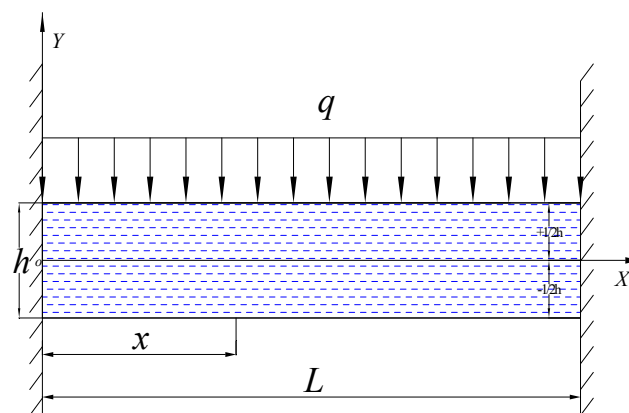


Figure 2. Schematic diagram of the key stratum fixed beam model.

The bending moment of any cross-section inside the rock beam of the key stratum can be expressed as [35]:

$$M_x = \frac{q}{12} (6Lx - 6x^2 - L^2) \quad (9)$$

In the formula:

M_x is the bending moment of any cross-section x in rock beam, Pa·m²;

L is the span of the rock beam, m;

q is the rock beam load of the key stratum, Pa;

h is the thickness of the rock beam, m.

Therefore, the maximum bending moment at both ends of the beam is:

$$M_{\max} = \frac{qL^2}{12} \quad (10)$$

The central bending moment of the beam is:

$$M_{\max} = \frac{qL^2}{24} \quad (11)$$

According to mechanics, the failure of this rock beam is tensile failure. Assuming that the thickness of the rock beam is h , the normal stress σ of the beam upper and lower boundary y ($y = \pm \frac{1}{2}h$) is:

$$\sigma = \frac{12M_y}{h^3} = \pm \frac{q}{2h^2} (6Lx - 6x^2 - L^2) \quad (12)$$

The maximum stress at both ends of the beam is:

$$\sigma_{\max} = \frac{qL^2}{2h^2} \quad (13)$$

From Formula (13), the initial limit breaking distance of the i -th key stratum is:

$$L_i = h_i \sqrt{\frac{2\sigma_i}{q_i}} \quad (14)$$

In the formula:

L_i is the initial limit breaking distance of the i -th key stratum;

σ_i is the maximum tensile strength stress of the i -th key stratum;

h_i is the thickness of the i -th key stratum;

q_i is the load of the i -th key stratum above.

As the workplace continues to advance, the overburden roof breaks and falls for the first time. The workplace will break and collapse periodically. The period collapse step distance L_p is calculated by the Formula (15):

$$L_p = 2h_i \sqrt{\frac{\sigma_i}{3q_i}} \quad (15)$$

3. Results

3.1. Engineering Background

The study area selected is the Daliuta coal mine, which belongs to the mining area under the jurisdiction of Shendong Coal Industry Group. It is located on the Ulan Mulun River in the town of Daliuta, Shenmu County, Yulin City, Shanxi Province, China, which borders Ordos City in the Inner Mongolia Autonomous Region. This mine is one of China's most supersized and high yield mines, with an annual output of more than 21 million tons. Figure 3 shows its geographic location. A northwesterly wind prevails in spring and winter in the study area, with a speed of approximately 3.3 m/s. The annual average precipitation is less than 400 mm, and the annual variation is considerable. Sixty percent of the annual precipitation is mainly concentrated in July–September. This study area is located in a temperate semiarid desert plateau continental monsoon climate [36]. In the study area, there is a TAS layer covering the ground.

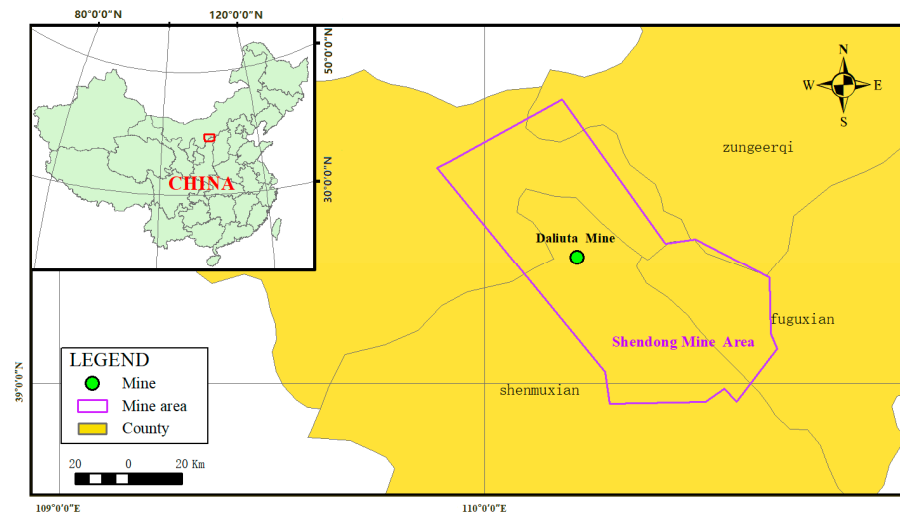


Figure 3. Geographical location of the study area.

During the advancement of the workface, there were many dense cracks on the surface of the Daliuta mining area, showing discontinuity and some regularity. Various types of surface cracks appear on the surface, which appear in the range of 10–100 m on the surface in front of the working face. These cracks can be subdivided into tensile cracks, compression cracks and stepped cracks. Different directions of stress can be analyzed through the crack shape on the surface. According to the data, the surface damage characteristics of the Daliuta mining area are as follows: tensile cracks appear on the surface in front of the workface, with a width of 0.3–0.5 m. The step crack drop is approximately 0.4–0.9 m, the maximum depth is approximately 3.5 m, and the crack spacing is only 2–3 m. The distribution density and width of compression cracks are slightly smaller than those of tensile cracks. Compression cracks with a length of 30–50 m appear at intervals of 2–3 m, and the uplift height is approximately 0.6 m.

Workface 1203 in the Daliuta mine was taken as the research object. The ground elevation of this workface is from 1083.4 m to 1229.3 m, and the coal seam floor elevation is from 981.3 m to 1032.8 m. The burial depth of the coal seam is 82–247 m, with an inclination angle of 1–3°, and the average burial depth of the coal seam is 90.3 m. The mining average thickness of the coal seam is designed to be 6.7 m. The surface above the workface is mostly covered by Quaternary loose sediment and mainly includes aeolian sand, with a thickness of 38.5 m. A bedrock layer with a thickness of approximately 51.8 m is mainly composed of siltstone mixed with sandy mudstone, coarse grained sandstone and fine grained sandstone. The coal floor is a fine grained sandstone layer with thickness of more than 3.0 m. The mining size of the workface is designed to be 301.3 m wide, and the advancing distance is 4268.8 m long. It adopts a fully mechanized and fully caving mining method with a large mining height and long working face. This high intensity mining method will lead to severe ground damage, such as subsidence, cracks, and even collapse pits.

3.2. Numerical Simulation Model Establishment

To more clearly study the principle of surface damage and rock stratum failure, a numerical simulation method was used to simulate and analyze the study area. The actual cause of surface cracks and damage is the surface subsidence caused by the mining process. However, the surface subsidence is caused by the settlement and damage of bedrock. The failure essence of the overburden lies in the failure of key stratum. The mechanical nature of the key stratum failure is the direct expression and essence of the surface and overburden failure. The numerical simulation method is a mechanical analysis method that can reflect the essential regular pattern of things, which is well recognized and practiced. Therefore, we use the numerical simulation method to analyze the overburden

and surface damage caused by the mining of SBTCS and find the essential regular pattern of overburden damage.

FLAC3D software was selected to calculate the numerical model based on the geological conditions of the 1203 workface in the Daliuta Coal Mine. Tecplot software was used for drawing processing in the later stage. With the Mohr–Coulomb mechanics constitutive model, a numerical calculation 3D model was established for mining SBTCS under TAS [37,38]. The models in the X, Y and Z directions are 1000 m, 500 m and 100 m, respectively, with a total of 5,000,000 zones and six groups, as shown in Figure 4. Ensuring the mining size is as close to the real size as possible and reducing the influence of edge effects, 100 m coal pillars are reserved around the workface without mining. Due to a large number of nodes in the model, a high performance calculation is needed. The data solution takes a long time to reach the final mechanical equilibrium state.

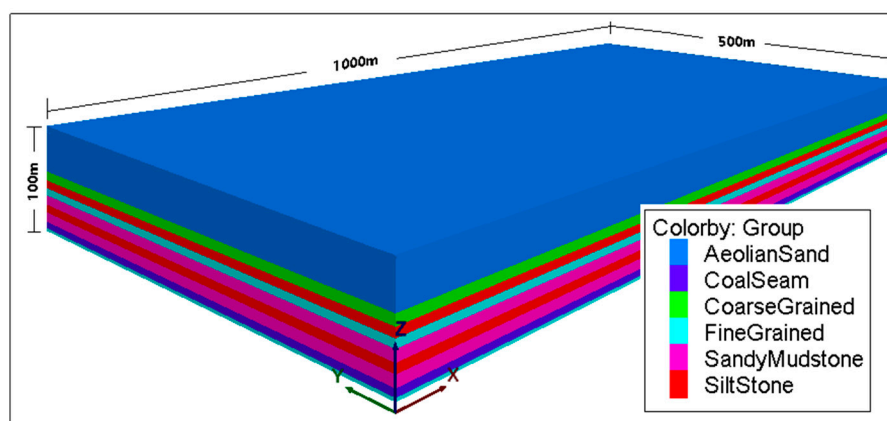


Figure 4. Schematic diagram of the 3D model of the numerical simulation based on FLAC3D.

To simulate the original stress of the underground rock stratum well, the model's boundary conditions must be limited to ensure that the model more truly reflects the actual geological conditions. The periphery of the model was fixed in the X and Y directions, to ensure that the boundary of the simulated stratum was not deformed in the horizontal direction. The bottom was completely fixed in the vertical Z direction, and the top was a free boundary, as shown in Figure 5. Mechanical parameters are the most important in the process of numerical simulation [39]. For the simulation of initial in situ stress, in FLAC, the initial stress is usually solved by setting the mechanical parameters and then solving to equilibrium. The original parameters are assigned according to the mechanical properties of the strata of the borehole. Under the action of gravity only, the initial in situ stress is solved to equilibrium (unbalance rate 10^{-6}). The selection and adjustment of the constitutive model and parameters is an essential link in numerical simulation. The selection of the constitutive model is related to the mechanical properties of the rock stratum, and the number and value of the corresponding parameters need to be selected for different constitutive models. The main mechanical parameters in the model came from the geological conditions of the Daliuta 1203 workface for calculating the stress in the numerical simulation. The physical and mechanical parameters of the rock stratum in the numerical simulation are shown in Table 1.

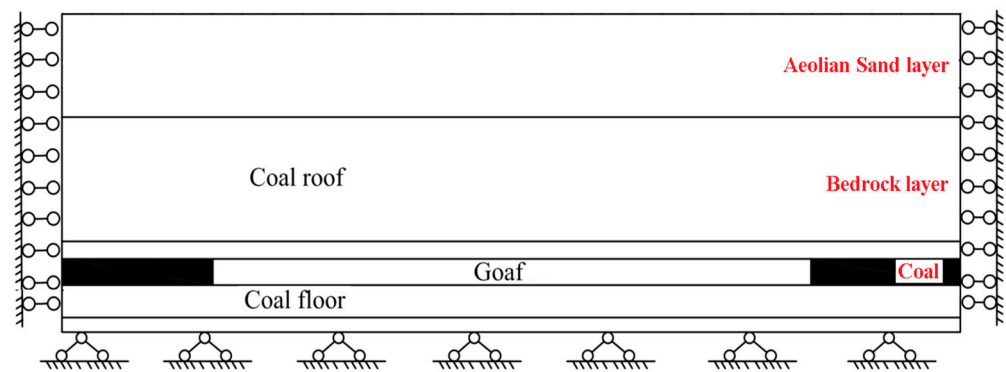


Figure 5. Boundary conditions of the 3D model for numerical simulation.

Table 1. Rock mechanics parameters in numerical simulation.

Lithology	h/m	E/Gpa	ρ	$\gamma/kN/m^3$	R_m/Mpa	c/Mpa	$\varphi/^\circ$
Aeolian Sand	38.5	12	0.3	15.8	0.0048	0.0016	27
Coarse Grained Sandstone	9.0	35	0.25	21	2.3	3.2	54
Siltstone	8.0	35	0.25	25	2.1	2.74	39
Fine Grained Sandstone	7.2	32	0.25	24.6	2.8	5.72	49
Sandy Mudstone	9.7	23	0.28	24.6	3.5	2.8	29
Siltstone	8.1	35	0.25	25	2.3	2.74	39
Sandy Mudstone	9.8	23	0.28	24.6	3.5	2.8	29
Coal	6.7	15	0.35	22.5	0.6	0.8	38
Fine Grained Sandstone	3.0	32	0.28	24.6	2.8	5.72	49

According to the key stratum theory, determining the key stratum position requires multiple and cyclic calculations. In the calculation process, if the collapse distance of the $i - 1$ th stratum is smaller than the i th stratum, the load of the $i - 1$ th stratum should be added to the i th stratum. Recalculate until the fracture distance of the $i + 1$ th stratum is smaller than that of the i th stratum. The i th stratum is the key stratum. Using Formulas (14) and (15), the initial breaking and periodic fracture distances are calculated. According to the rock mechanics parameters in Table 1, we can calculate that the first key stratum is sandy mudstone, the immediate roof of coal. The initial failure distance is 52.85 m, and the periodic fracture distance is 43.12 m. Similarly, we can obtain that the second key stratum is sandy mudstone, which is between fine grained sandstone strata and siltstone strata. In the second key stratum, the initial failure distance is 56.37 m, and the periodic fracture distance is 46.03 m.

3.3. Analysis of Ground Damage and Field Measured Results

The simulation of the workface propulsion distance at 100 m, 200 m, 300 m, 400 m, 500 m, 600 m, 700 m and 800 m is extracted. According to different advancing distances, the settlement and stress changes in the surface and overburden are recorded as cloud maps. The cloud maps of the numerical simulation, such as the form of and change in ground damage, the settlement and stress distribution of the overburden, and the shape and field of plastic failure, are analyzed to obtain the failure characteristics of the overburden and surface movement and deformation.

For calibration and validation of the model, to obtain surface subsidence change data of SBTCS, the 46 monitoring points, where the distance between monitoring points is set to 20–25 m, with 21.7 m on average, were set up on the surface above the ground and monitored the settlement. Surface monitoring was carried out using traditional leveling methods. Two vertical observation lines were arranged along the ground to obtain the surface subsidence under the condition of different working face advancing distances, and then the subsidence caused by mining of SBTCS was analyzed. When the workface advanced by approximately 600 m, we selected 21 points for trend analysis between

measured points and simulated calculated points. The maximum settlement of the surface was -3.898 m. The ground settlement, which was calculated by FLAC 3D, reached the maximum value of -3.78544 m (the data measured in the field and calculated by FLAC3D are shown in Figure 6). The resulting error ratio is about 2.89%. Through a comparison, it was found that the surface settlement value of the numerical simulation was very close to the field measured. The surface subsidence trend line is also in good agreement. This shows that the numerical simulation method is an effective method to calculate and predict the surface settlement caused by coal mining by establishing a reasonable 3D model, selecting an appropriate constitutive model and adjusting the corresponding mechanical parameters.

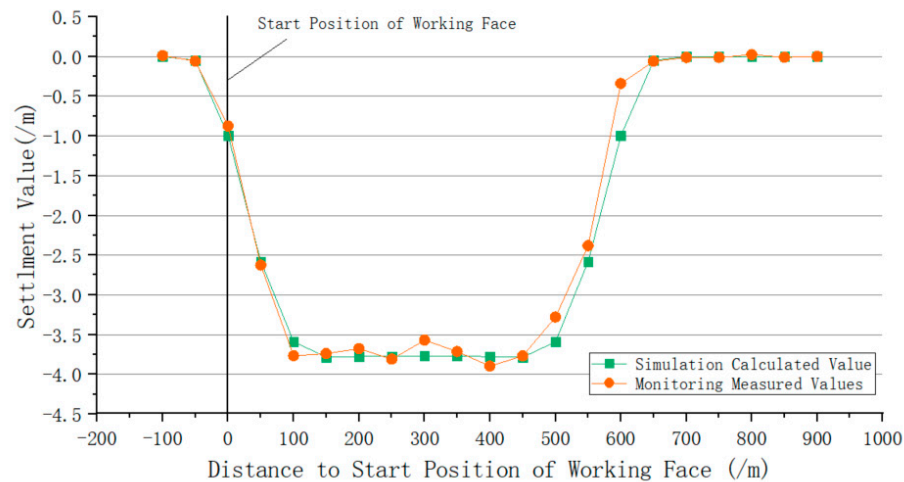


Figure 6. Comparison of calculated and measured values of ground subsidence.

Through numerical simulation, the shape of the surface subsidence basin is very close to the actual field. The subsidence at the edge of the basin is small, and there is more subsidence in the middle, which has a flat bottom. According to Figure 7, the settlement of the bedrock is large, and the settlement of the aeolian sand layer is small. There are large pores and cracks in the aeolian sand layer and the bedrock layer. The main reason is that aeolian sand has weak mechanical properties and good dispersion, and easily forms pores. The mechanical properties of the overburden are hard, brittle and easily broken, and collapsed. The settlement cloud map of the bedrock above the goaf shows that the settlement in the center is large and that along the edge it is smaller. The simulation calculation of the overburden settlement shows that the overburden failure caused by mining SBTCS under TAS has distinctive characteristics. The bedrock in the overburden generally has large settlements and has a large scale overall movement phenomenon, and the maximum subsidence is more than 6.5 m. The aeolian sand layer presents uniform settlement, the maximum subsidence is 3.5–4.0 m in the central basin. The movement and deformation in the central subsidence basin show uniform settlement and little change. With increasing mining distance, the surface subsidence gradually increases. When the working advance is approximately 300 m, it is close to full-mining under these geological conditions. Then, with the advance of mining distance, the ground subsidence basin appears to a flat bottom [40].

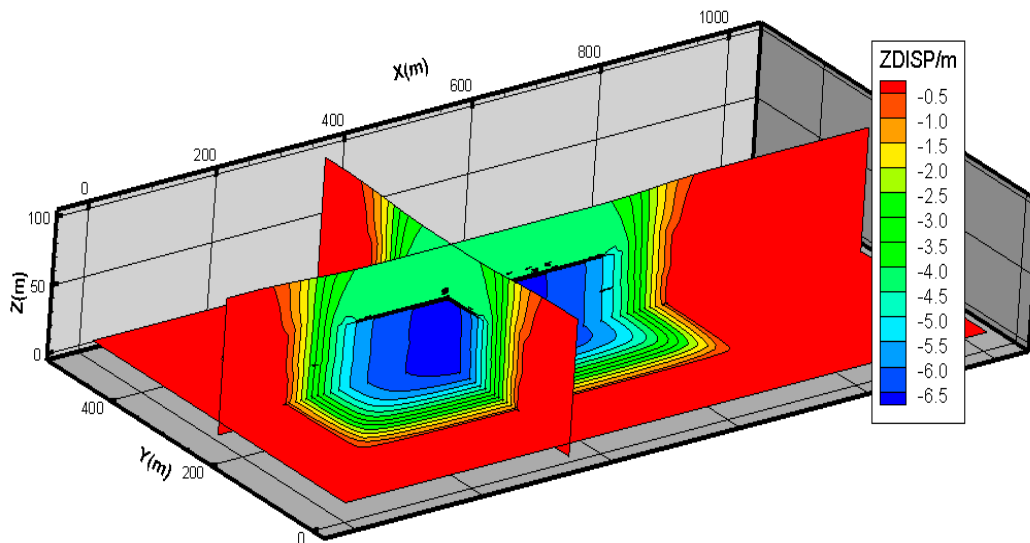


Figure 7. Cloud map of Deformation characteristics of overburden settlement.

As shown in Figure 8, many cracks are generated on the ground surface before and on both sides of the workface affected by mining. The surface has distinct damage. The cracks in front of the workface probably range from 20 m to 240 m, and the distance of crack is approximately 10–80 m.

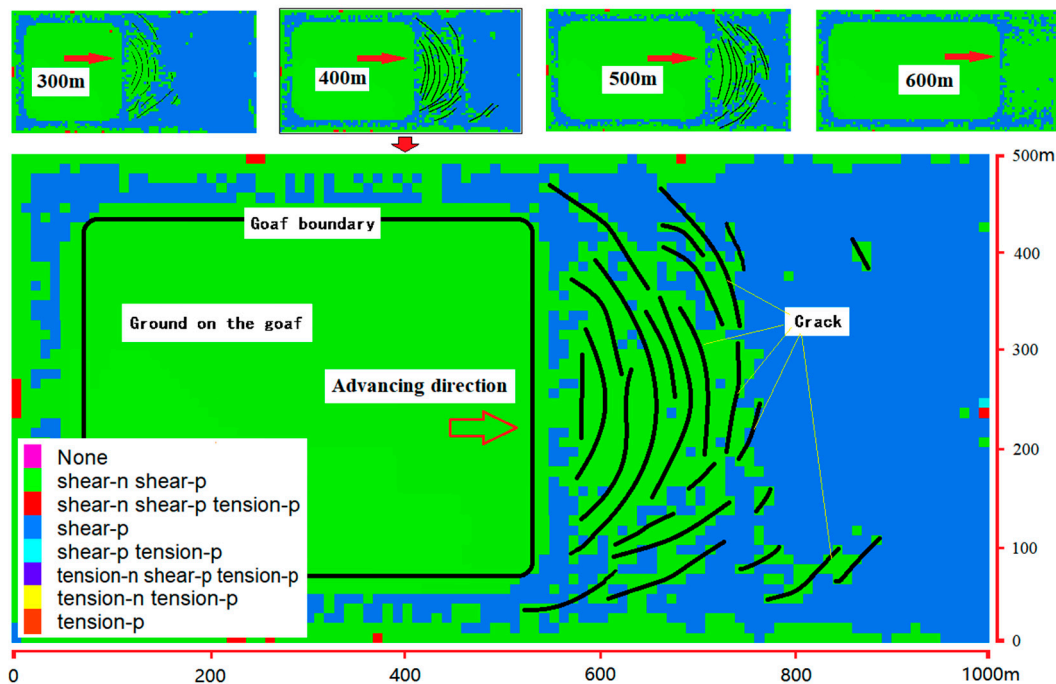


Figure 8. Deformation characteristics of ground.

3.4. Overburden Failure Analysis

With the continuous advancement of the working face, the roof of the coal seam collapses, and the collapsed rock fragments are superimposed on the goaf to form a masonry beam structure, the surface begins to subside, and the overburden under the aeolian sand begins to crack or even fracture. Finally, the original stress balance of the overburden, which is affected by mining, is broken.

A stress concentration phenomenon occurs in the overburden above the edge of the goaf that are affected by mining, as shown in Figure 9. After the collapse of the first key

stratum, the second key stratum plays a major supporting role. The maximum vertical stress is more than 9.0 MPa and the direction is downward, and its support point moves upward, and such disasters caused by high stress often cause great damage to mining engineering activities [3,41,42]. An interlayer with weak stress appears between the aeolian sand layer and the bedrock layer. The reason for this is maybe that, after the mechanical state of bedrock layers and aeolian sand layer changes caused by mining, cracks and separation layers are generated between them.

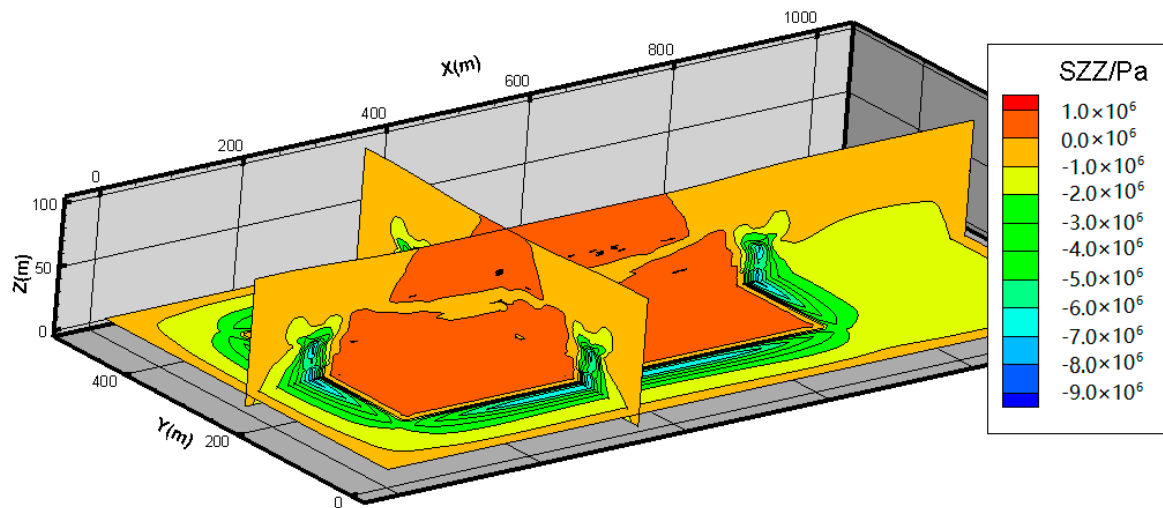


Figure 9. Cloud map of the overburden stresses.

As shown in Figure 10, shear failure and tensile failure show a layered structure in the horizontal direction and alternately appear in the vertical direction. The upper aeolian sand is mainly sheared, and the lower of aeolian sand is mainly tensile failure. The movement angle is different in the aeolian sand layer and the bedrock layer. The movement angle of the aeolian sand layer is smaller, while the movement angle of the bedrock layer is larger [43]. The movement angle in the TAS layer is smaller than that in the bedrock, which enlarges the range of the subsidence basin and expands the scope of ground damage.

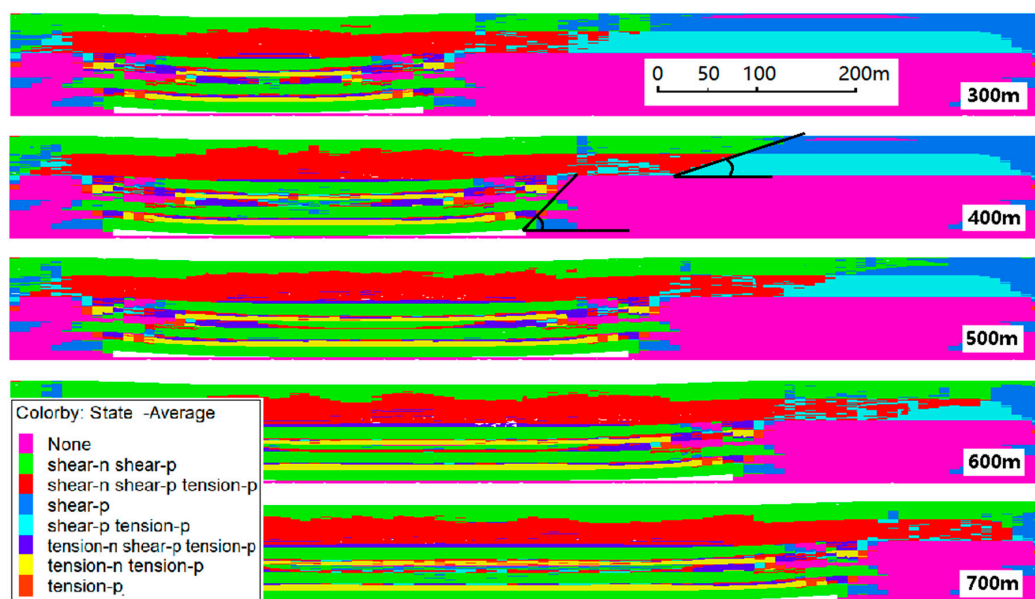


Figure 10. Plastic deformation of overburden at different schedule.

Overburden collapse can be divided into two stages, initial collapse and periodic collapse, as shown in Figure 11. The initial fracture distance is usually larger than the periodic fracture distance. After the initial collapse, with the advance of the working face, the overburden forms a cantilever structure. When the maximum bearing capacity is reached, periodic collapse occurs. Then, the overburden directly collapses to the goaf, the height of the collapse zone is approximately 24 m. The collapse block is 40–50 m long, and it is consistent with the theoretical calculation. The collapse block is gradually crushed and compacted. The block provides a bearing capacity to support the upper broken key stratum.

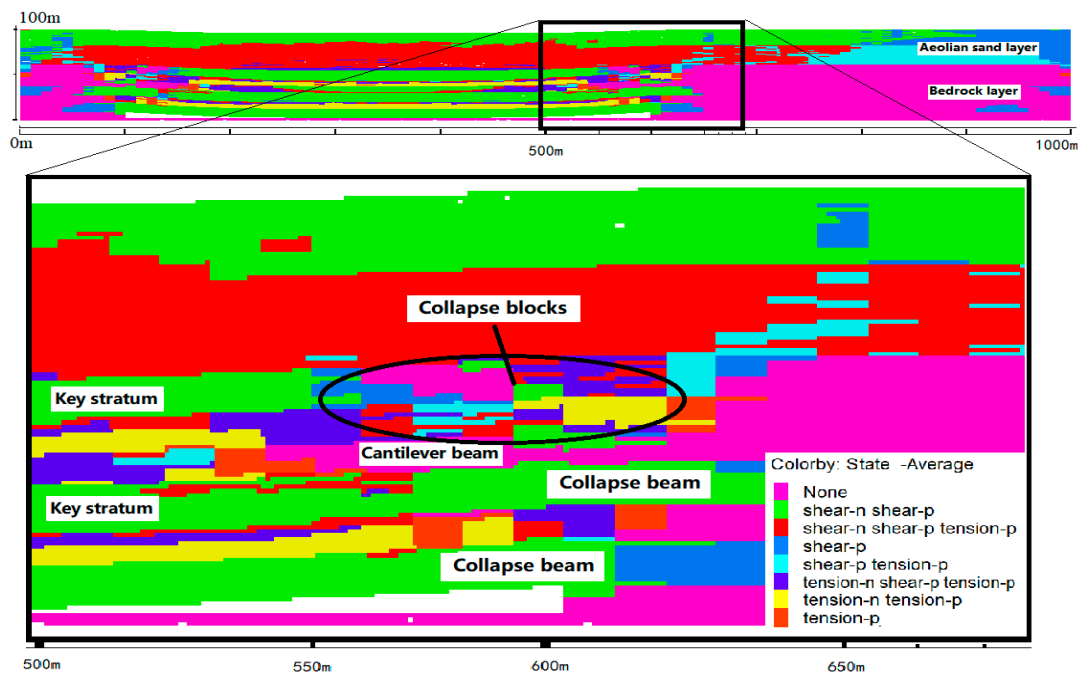


Figure 11. Local enlarged schematic diagram of key stratum collapse and cantilever beam formation process.

According to the cloud map of the numerical simulation, under this geological condition. The key stratum exists in the form of “cantilever beam” before collapse and “masonry beam” after collapse. There are a large number of fractures and fissures between blocks. With the continuous advancement of the working face, cracks in the overburden stratum continue to develop, and run through the whole bedrock layer, and there is no “bending zone” in the overburden. The cracks directly connect to the surface and form conduction with the surface.

4. Discussion

In this paper, we show that the overburden failure caused by the mining SBTCS, when the ratio of depth to thickness is less than 15 ($H/h = 13.43$), can be divided into two stages: initial collapse and periodic collapse. According to the theoretical calculation, the initial collapse distance is greater than the collapse step, approximately 55 m on average, and the collapse step is approximately 45 m on average in the Daliuta Coal Mine.

The results of theoretical calculations are within the range of numerical simulation results. The movement angle in the loose thick aeolian sand layer is small, which expands the range of surface damage. A weak stress interlayer is generated between the overburden and the aeolian sand layer. This may be the cause of much shear, tension and compression failure on the ground, as shown in Figure 12. This study provides a mechanical analysis basis for the surface damage caused by mining shallow and thick coal seams, and provides a basis for surface environmental treatment and ecological restoration.

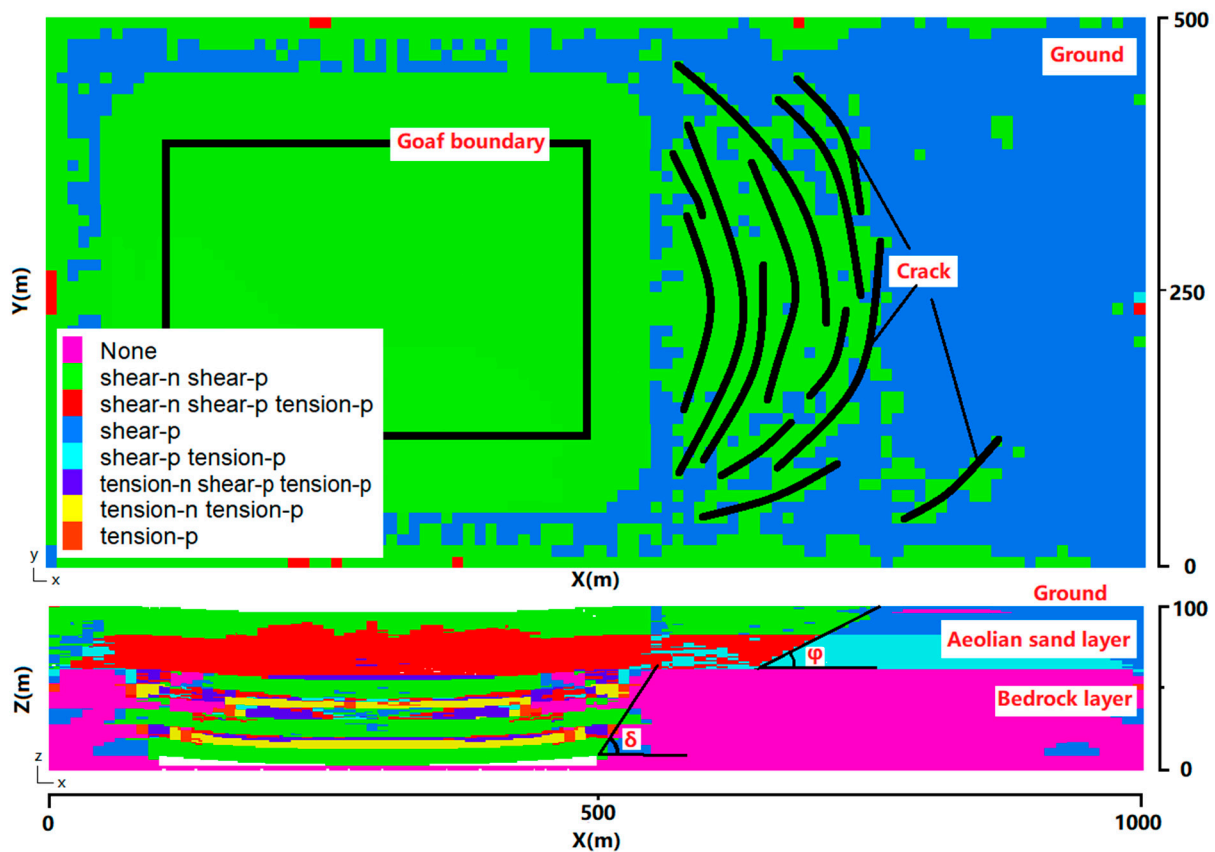


Figure 12. Comparison between overburden failure and surface failure.

The study of coal mine surface damage can improve our understanding of mine management and land reclamation, and be conducive to ecological mine restoration. The research on mining SBTCS has strong regional characteristics. In different geological conditions and rock stratum conditions, resulting overburden and surface damage also have different status [43–45]. Hou [34] and Huang [33] adopt the same calculation method as our study. Huang studies the failure mechanism of mining shallow coal seams and uses the result to control the ground pressure. Hou adopts the key stratum theory, puts forward the method of composite rock beams, and calculates the relevant parameters of rock beams. Although the stratigraphic conditions are quite different, the methods and ideas of theoretical analysis are correct. The study area and environment in Zou [4] is very close to our study. They obtained the conclusion that overburden failure presents periodic collapse and initial collapse, which is consistent with this study. However, we further analyzed the stress distribution characteristics of overburden and the variation regular pattern of movement angle in loose layers and bedrock layers.

The study area is located in an arid desert area in China. The influence of groundwater on overburden is not considered in this study. The study of the interaction between overburden and groundwater is a complex and long term process. Through the monitoring of surface water level, overburden pore water pressure and overburden stress change, the interaction relationship between overburden and water can be obtained, the coupling model of overburden failure and groundwater can be established, and the interaction relationship between overlying rock and groundwater can be obtained. The occurrence conditions and geological structure of coal seams in the study area are simple, belonging to horizontal coal seams with few faults. For complex geological conditions, such as coal seam dip angle and faults, further research will be carried out later in the research process. When there are dip angles and faults in overburden and coal seams, a variety of numerical simulation models with different dip angles and different fault forms can be constructed by simulation to study the characteristics of overburden and surface failure under complex

conditions from the perspective of numerical simulation. According to mining subsidence theory and mechanical theory [44–46], the surface damage range can be calculated more accurately rather than qualitative analysis. When mining SBTCS, the DTR and aeolian sand thickness to bedrock thickness ratio (ASBR) should be considered. It reflects the relationship between coal seam thickness and buried depth, and the structural composition of bedrock. The change in DTR and ASBR have a key impact on the overburden and surface damage caused by mining SBTCS, which is also a subject worthy of in depth study in the future.

5. Conclusions

Based on the theory of key stratum and elastic mechanics, a mechanics model of key stratum failure was established in mining SBTCS under TAS. We calculated the breaking distance and periodic step distance of overlying strata. The key stratum were simplified as a fixed supporting beam structure to simplify the calculation formula. By calculation, we found that the initial failure distance is 52.81 m and the periodic breaking step distance is 43.12 m in the first key stratum. The initial failure distance is 56.37 m, and the periodic breaking step distance is 46.03 m in the second key stratum in Daliuta Coal Mine.

- (1) According to the geological engineering conditions of the 1203 workface in the Daliuta Coal Mine, a numerical model was established by FLAC3D software. Compared with the field monitoring data of the surface, the numerical simulation results are very close to the measured values (the difference between the measured maximum settlement value and the simulated maximum settlement value is 0.11256 m (error accounts for 2.89%)). By correctly selecting the constitutive model and adjusting the appropriate parameters, the numerical simulation method is a method based on theoretical calculation, which can calculate and predict surface dependency caused by coal mining.
- (2) The results show many cracks on the surface in front of the workface, which probably range from 240 m to 20 m. The distance between cracks is approximately from 10–80 m. The reason for the cracks on the ground is that the settlement of bedrock entirely exceeds that of the aeolian sand layer, and the shear stress of the aeolian sand layer by mining SBTCS.
- (3) Although our research has achieved some results, we will further study and discuss the coupling effect of overburden and water, complex geological conditions and the influence of DTR on SBTCS.

Author Contributions: Conceptualization, Y.Z. and J.C.; methodology, Y.Z.; software, G.L.; validation, W.Z., G.L. and Y.Z.; formal analysis, G.L.; investigation, W.Z.; resources, W.Z.; data curation, G.L.; writing—original draft preparation, G.L.; writing—review and editing, G.L. and W.Z.; visualization, G.L.; supervision, W.Z.; project administration, W.Z.; funding acquisition, Y.Z. All authors have read and agreed to the published version of the manuscript.

Funding: This research was funded by the National Natural Science Foundation of China, grant number U1810203 and U21A20108, and This research was funded by Henan province science and technology tackling key project, China, grant number 212102310404.

Institutional Review Board Statement: Not applicable.

Informed Consent Statement: Not applicable.

Data Availability Statement: The data used to support the findings of this study are included within the article.

Conflicts of Interest: The authors declare no conflict of interest.

References

1. Dong, L.; Hu, Q.; Tong, X.; Liu, Y. Velocity-Free MS/AE Source Location Method for Three-Dimensional Hole-Containing Structures. *Engineering* **2020**, *6*, 827–834. [[CrossRef](#)]
2. Helm, P.R.; Davie, C.T.; Glendinning, S. Numerical modelling of shallow abandoned mine working subsidence affecting transport infrastructure. *Eng. Geol.* **2013**, *154*, 6–19. [[CrossRef](#)]

3. Dong, L.; Tong, X.; Ma, J. Quantitative Investigation of Tomographic Effects in Abnormal Regions of Complex Structures. *Engineering* **2020**, *7*, 1011–1022. [[CrossRef](#)]
4. Zou, Y. *Evolution Mechanism and Regulation of Surface Ecological Environment under High Intensity Mining*; Science Press: Beijing, China, 2019.
5. Yang, X.; Wen, G.; Dai, L.; Sun, H.; Li, X. Ground Subsidence and Surface Cracks Evolution from Shallow-Buried Close-Distance Multi-seam Mining: A Case Study in Bulianta Coal Mine. *Rock Mech. Rock Eng.* **2019**, *52*, 2835–2852. [[CrossRef](#)]
6. Ma, C.; Cheng, X.; Yang, Y.; Zhang, X.; Guo, Z.; Zou, Y. Investigation on Mining Subsidence Based on Multi-Temporal InSAR and Time-Series Analysis of the Small Baseline Subset—Case Study of Working Faces 22201-1/2 in Buertai Mine, Shendong Coalfield, China. *Remote Sens.* **2016**, *8*, 951. [[CrossRef](#)]
7. Li, Z.; Pang, Y.; Bao, Y.; Ma, Z. Research on Surface Failure Law of Working Faces in Large Mining Height and Shallow Buried Coal Seam. *Adv. Civ. Eng.* **2020**, *2020*, 8844249. [[CrossRef](#)]
8. Alejano, L.R.; Taboada, J.; García-Bastante, F.; Rodriguez, P. Multi-approach back-analysis of a roof bed collapse in a mining room excavated in stratified rock. *Int. J. Rock Mech. Min. Sci.* **2008**, *45*, 899–913. [[CrossRef](#)]
9. Kapusta, K.; Stańczyk, K.; Wiatowski, M.; Češko, J. Environmental aspects of a field-scale underground coal gasification trial in a shallow coal seam at the Experimental Mine Barbara in Poland. *Fuel* **2013**, *113*, 196–208. [[CrossRef](#)]
10. Park, D.; Michalowski, R.L. Three-dimensional roof collapse analysis in circular tunnels in rock. *Int. J. Rock Mech. Min. Sci.* **2020**, *128*, 104275. [[CrossRef](#)]
11. Bell, F.G.; Stacey, T.R.; Genske, D.D. Mining subsidence and its effect on the environment: Some differing example. *Environ. Geol.* **2000**, *40*, 135–152. [[CrossRef](#)]
12. Kontogianni, V.; Pytharouli, S.; Stiros, S. Ground subsidence, Quaternary faults and vulnerability of utilities and transportation networks in Thessaly, Greece. *Environ. Geol.* **2007**, *52*, 1085–1095. [[CrossRef](#)]
13. Howladar, M.F.; Hasan, K. A study on the development of subsidence due to the extraction of 1203 slice with its associated factors around Barapukuria underground coal mining industrial area, Dinajpur, Bangladesh. *Environ. Earth Sci.* **2014**, *72*, 3699–3713. [[CrossRef](#)]
14. Fan, D.Y.; Liu, X.S.; Tan, Y.L.; Song, S.L.; Ning, J.G.; Ma, Q. Numerical simulation research on response characteristics of surrounding rock for deep super-large section chamber under dynamic and static combined loading condition. *J. Cent. South Univ.* **2020**, *27*, 3544–3566. [[CrossRef](#)]
15. Li, M.; Zhang, J.X.; Huang, Y.L.; Gao, R. Measurement and numerical analysis of influence of key stratum breakage on mine pressure in top-coal caving face with super great mining height. *J. Cent. South Univ.* **2017**, *24*, 1881–1888. [[CrossRef](#)]
16. Sepehri, M.; Apel, D.B.; Hall, R.A. Prediction of mining-induced surface subsidence and ground movements at a Canadian diamond mine using an elastoplastic finite element model. *Int. J. Rock Mech. Min. Sci.* **2017**, *100*, 73–82. [[CrossRef](#)]
17. Jawed, M.; Sinha, R.K. Design of rhombus coal pillars and support for Roadway Stability and mechanizing loading of face coal using SDLs in a steeply inclined thin coal seam—A technical feasibility study. *Arab. J. Geosci.* **2018**, *11*, 415. [[CrossRef](#)]
18. Unver, B.; Yasitli, N.E. Modelling of strata movement with a special reference to caving mechanism in thick seam coal mining. *Int. J. Coal Geol.* **2006**, *66*, 227–252. [[CrossRef](#)]
19. Zhu, H.Z.; Liu, P.; Tong, Z.Y. Numerical simulation research and application on protected layer pressure relief a ction under different coal pillar width. *Procedia Eng.* **2014**, *84*, 818–825.
20. Salmi, E.F.; Nazem, M.; Karakus, M. Numerical analysis of a large landslide induced by coal mining subsidence. *Eng. Geol.* **2017**, *217*, 141–152. [[CrossRef](#)]
21. Das, R.; Singh, P.K.; Kainthola, A.; Panthee, S.; Singh, T.N. Numerical analysis of surface subsidence in asymmetric parallel highway tunnels. *J. Rock Mech. Geotech. Eng.* **2017**, *9*, 170–179. [[CrossRef](#)]
22. Ghabraie, B.; Ren, G.; Zhang, X.; Smith, J. Physical modelling of subsidence from sequential extraction of partially overlapping longwall panels and study of substrata movement characteristics. *Int. J. Coal Geol.* **2015**, *140*, 71–83. [[CrossRef](#)]
23. Liu, W.; Pang, L.; Xu, B.; Sun, X. Study on overburden failure characteristics in deep thick loose seam and thick coal seam mining. *Geomat. Nat. Hazards Risk* **2020**, *11*, 632–653. [[CrossRef](#)]
24. Zhang, J.; Li, F.; Zeng, L.; Peng, J.; Li, J. Numerical simulation of the moisture migration of unsaturated clay embankments in southern China considering stress state. *Bull. Eng. Geol. Environ.* **2021**, *80*, 11–24. [[CrossRef](#)]
25. Booth, C.J. *The Effects of Longwall Coal Mining on Overlying Aquifers*; Special Publications; Geological Society: London, UK, 2002.
26. Dai, H.; Lian, X.; Liu, J.; Liu, Y.; Zhou, Y.; Deng, W.; Cai, Y. Model study of deformation induced by fully mechanized caving below a thick loess layer. *Int. J. Rock Mech. Min. Sci.* **2010**, *47*, 1027–1033. [[CrossRef](#)]
27. Sheorey, P.R.; Loui, J.P.; Singh, K.B.; Singh, S.K. Ground subsidence observations and a modified influence function method for complete subsidence prediction. *Int. J. Rock Mech. Min. Sci.* **2000**, *37*, 801–818. [[CrossRef](#)]
28. Ghabraie, B.; Ren, G.; Barbato, J.; Smith, J.V. A predictive methodology for multi-seam mining induced subsidence. *Int. J. Rock Mech. Min. Sci.* **2017**, *93*, 280–294. [[CrossRef](#)]
29. Wang, J.C.; Jiang, F.X.; Meng, X.J.; Wang, X.Y.; Zhu, S.T.; Feng, Y. Mechanism of Rock Burst Occurrence in Specially Thick Coal Seam with Rock Parting. *Rock Mech. Rock Eng.* **2016**, *49*, 1953–1965. [[CrossRef](#)]
30. Wang, T.; Ikarashi, K. Post Local Buckling Behavior and Ultimate Capacity of H-section Beam. *J. Asian Archit. Build. Eng.* **2011**, *10*, 429–436. [[CrossRef](#)]
31. Qian, M.; Miao, X.; Xu, J. Theoretical study on key stratum in strata control. *J. China Coal Soc.* **1996**, *21*, 12–23.

32. Xu, J.; Qian, M. Method for identifying the location of key overburden layers. *J. China Univ. Min. Technol.* **2000**, *29*, 463–467.
33. Huang, S. *Research on the Damage Mechanism and Control Methods of Cracks Caused by Mining in Shallow Coal Seams*; Xi'an University of Science and Technology: Xi'an, China, 2006; pp. 50–55.
34. Hou, Z. Application of combined key stratum theory and determination of its parameters. *Acta Coalae Sin.* **2001**, *26*, 611–615.
35. Li, H.; Yang, J.; Liu, M. Elastoplastic analysis of fixed beams at both ends under uniformly distributed load. *J. Hehai Univ. (Nat. Sci. Ed.)* **2005**, *4*, 447–451.
36. Liu, W.; Pang, L.; Liu, Y.; Du, Y. Characteristics Analysis of Roof Overburden Fracture in Thick Coal Seam in Deep Mining and Engineering Application of Super High Water Material in Back fill Mining. *Geotech. Geol. Eng.* **2019**, *37*, 2485–2494. [[CrossRef](#)]
37. Fujii, Y.; Ishijima, Y. Numerical simulation of microseismicity induced by deep longwall coal mining. *Min. Sci. Technol.* **1991**, *12*, 265–285. [[CrossRef](#)]
38. Eberhardt, E. The Hoek-Brown failure criterion. *Rock Mech. Rock Eng.* **2012**, *45*, 981–988. [[CrossRef](#)]
39. Swift, G. Relationship between joint movement and mining subsidence. *Bull. Eng. Geol. Environ.* **2014**, *73*, 163–176. [[CrossRef](#)]
40. Marschalko, M.; Yilmaz, I.; Lamich, D.; Drusa, M.; Kubečková, D.; Peňaz, T.; Burkotová, T.; Slivka, V.; Bednárik, M.; Krčmář, D.; et al. Unique documentation, analysis of origin and development of an undrained depression in a subsidence basin caused by underground coal mining (Kozinec, Czech Republic). *Environ. Earth Sci.* **2014**, *72*, 11–20. [[CrossRef](#)]
41. Alencar, A.; Galindo, R.; Melentijevic, S. Influence of the groundwater level on the bearing capacity of shallow foundations on the rock mass. *Bull. Eng. Geol. Environ.* **2021**, *80*, 6769–6779. [[CrossRef](#)]
42. Yan, W.; Chen, J.; Tan, Y.; Zhang, W.; Cai, L. Theoretical analysis of mining induced overburden subsidence boundary with the horizontal coal seam mining. *Adv. Civ. Eng.* **2021**, *2021*, 6657738. [[CrossRef](#)]
43. Unlu, T.; Akcin, H.; Yilmaz, O. An integrated approach for the prediction of subsidence for coal mining basins. *Eng. Geol.* **2013**, *166*, 186–203. [[CrossRef](#)]
44. Chen, C.; Hu, Z.; Wang, J.; Jia, J. Dynamic Surface Subsidence Characteristics due to Super-Large Working Face in Fragile-Ecological Mining Areas: A Case Study in Shendong Coalfield, China. *Adv. Civ. Eng.* **2019**, *2019*, 8658753. [[CrossRef](#)]
45. Sun, Y.; Zuo, J.; Karakus, M.; Wen, J. A Novel Method for Predicting Movement and Damage of Overburden Caused by Shallow Coal Mining. *Rock Mech. Rock Eng.* **2020**, *53*, 1545–1563. [[CrossRef](#)]
46. Yu, X.Y.; Wang, P.; Li, X.L. Analysis on characteristics of surface subsidence with Han Jia Wan coal mine. *Adv. Mater. Res.* **2012**, *524*, 520–527. [[CrossRef](#)]